

Predicting the properties of black holes merger remnants with Deep Neural Networks

L. Haegel¹ and S. Husa¹

¹University of Balearic Islands

Abstract

We present the first estimation of the mass and spin of Kerr black holes resulting from the coalescence of binary black holes using a deep neural network. The network is trained on the full publicly available catalog of numerical simulations of gravitational waves emission by binary black hole systems. The network prediction for non-precessing binaries as well as precessing binaries is compared with existing fits in the LIGO-Virgo software package when existing. For the non-precessing case, the absolute error distribution has a root mean square error of $2.6 \cdot 10^{-3}$ for the final mass (twice lower than the existing fits) and $3 \cdot 10^{-3}$ for the final spin (similarly to the existing fits). We also estimate of the final mass in the precessing case, where we obtain a RMSE of $1 \cdot 10^{-3}$ of the absolute error distribution. It is $8 \cdot 10^{-3}$ when predicting the spin of the black hole resulting from a precessing binary, against $1.1 \cdot 10^{-2}$ for the existing fits.

1 Introduction

General relativity predicts that binary systems of black holes (BHs) coalesce by emitting gravitational waves (GWs). During the first two observational runs of advanced LIGO [1, 2] and advanced Virgo [3], GWs from ten binary black holes (BBHs) mergers have been detected [4]. Current GW instruments detect solar-masses BBHs in their late inspiral and merger phase of the coalescence, resulting in a Kerr BH characterized by its final mass M_f and final spin S_f . While the GW emission during the inspiral phase where the black holes separation is large can be computed in the post-Newtonian (PN) formalism [5], such perturbative methods are inadequate for the merging part that must be determined using numerical relativity (NR). Due to the high computational cost of NR simulations, a limited catalog of BBH

configurations is currently available. The information of the NR simulation must then be interpolated to cover the parameter space of the BH remnants detected by advanced LIGO and advanced Virgo. The relation between the initial BBH parameters and the remnant properties can be determined in fits based on the available NR simulations and interpolated to a wider range of parameters [6], that are notably necessary for the development of the phenomenological fits of full gravitational waveforms [7, 8]. The existing fits rely on explicit ansatz that may not capture fully the relationship between the initial and remnant properties, and may not be extendable to the high number of dimensions required to describe precessing BBHs. An accurate estimation of the remnant properties is of interest for fundamental physics, such as inspiral-merger-ringdown consistency tests aiming at testing the nature of the resulting BH [9]. They can also provide an estimate on the remnant parameters when only the inspiral part of the waveform is detected and the merger is outside the detection range, such as the case of small-masses BBHs for LIGO and Virgo.

In this article, we study the feasibility of using a deep neural network (DNN) to infer the relation between the initial BBHs parameters and the remnant final mass M_f and final dimensionless spin $\chi_f = S_f/M_f^2$. In addition to the interest in accurate models for the final state of BBH mergers, the present work can serve as an example of how to model other quantities of interest, and in principle the whole waveform, directly or in terms of the coefficients of some phenomenological model.

DNN are networks of nodes organized in layers, each node being assigned a weight that is propagated to the next layer according to a non-linear activation function. The first layer has the dimension of the input parameters size, while the last layer consists of one node returning the predicted output parameter. The weights of the DNN are adjusted with a backpropagation algorithm based on a stochastic gradient descent until the prediction is optimized. DNN have been shown to be powerful in extracting features from large datasets with high dimensionality, enabling to deliver accurate predictions on new data [10].

We train a DNN to estimate the final properties of the remnant for two sets of configuration, the first being non-precessing BBHs to compare the accuracy of the DNN prediction with the explicit fits, the second being precessing BBHs in order to estimate its accuracy on a parameter space of larger dimension. While the current remnant properties fits for precessing configurations available in the LIGO software library rely on aligned-spin configurations augmented by the in-plane spin component for the precessing case, our work is also motivated by the fact that Gaussian processes have shown to be powerful tools in estimating the remnant BH properties from the totality initial parameters, namely the masses and spin components [11]. Section 2 describes the NR and extreme mass ratio data used as input of

the DNN, while the fit procedure and results are given on Section 3 and discussed on Section 4.

2 Input data

2.1 Numerical relativity catalogs

The DNN are trained and tested with data from NR catalogs, in which the initial BBHs are characterized by their individual masses m_1 and m_2 with the convention $m_1 > m_2$. Since for BHs in general relativity the total mass acts as a simple scale factor, for simplicity we choose $m_1 + m_2 = 1$, and we parameterise the masses by the symmetric mass ratio $\eta = (m_1 m_2)/(m_1 + m_2)^2$. For the individual spins we introduce the dimensionless spins $\chi_{1,2} = S_{1,2}/m_{1,2}^2$ where S_1 and S_2 are the individual angular momenta. The remnant BH is defined by its final mass M_f and spin χ_f .

In the non-precessing case we follow [12] in parameterising the 2-dimensional spin parameter space by a dominant (“effective”) spin parameter $S_{eff} = (S_1 + S_2)/(1 - 2\eta)$ with the property $-1 \geq S_{eff} \geq 1$, and the spin difference $\Delta\chi = \chi_1 - \chi_2$. In the precessing case, we use two different sets of parameters. In what will be referred below as the *6d-parameterization*, we follow [13] where the input parameters are η , the total spins χ_1 and χ_2 , the tilt angles θ_1 and θ_2 and the planar spin projection angle difference ϕ_{12} as defined in equations (1) and (2):

$$\cos \theta_{1,2} = \frac{\overrightarrow{\chi_{1,2}} \cdot \overrightarrow{L_{1,2}}}{\|\overrightarrow{\chi_{1,2}}\| \|\overrightarrow{L_{1,2}}\|}, \quad (1)$$

$$\cos \phi_{12} = \frac{\overrightarrow{\chi_1^{plane}} \cdot \overrightarrow{\chi_2^{plane}}}{\|\overrightarrow{\chi_1^{plane}}\| \|\overrightarrow{\chi_2^{plane}}\|}, \quad (2)$$

where $\overrightarrow{\chi^{plane}} = \overrightarrow{\chi} - (\overrightarrow{\chi} \cdot \overrightarrow{L}) \overrightarrow{L}$ and \overrightarrow{L} is the angular momentum. We also train a DNN as a function of η , $\chi_{1\{x,y,z\}}$ and $\chi_{2\{x,y,z\}}$, set referred to as the *7d-parameterization*, in order to compare the prediction as a function of the input parameters.

DNNs are known to perform better when trained with large datasets, therefore all the publicly available NR catalogs have been used for the non-precessing fits, i.e. from the SpEC [11, 14–33], LaZev [34–44], MayaKranc [45] and BAM [46, 47] codes. In total, 1044 non-precessing NR simulations are used as summarized in Table 1. The following parameter ranges are covered: $\eta \in [0.050, 0.250]$, $S_{eff} \in [-0.970, 0.999]$, $\Delta\chi \in [-1.900, 1.861]$, $M_f \in [0.883, 0.997]$, $\chi_f \in [-0.527, 0.951]$. The distributions of the remnant parameters as a function of the symmetric mass ratio and effective spin is shown in Figure 1.

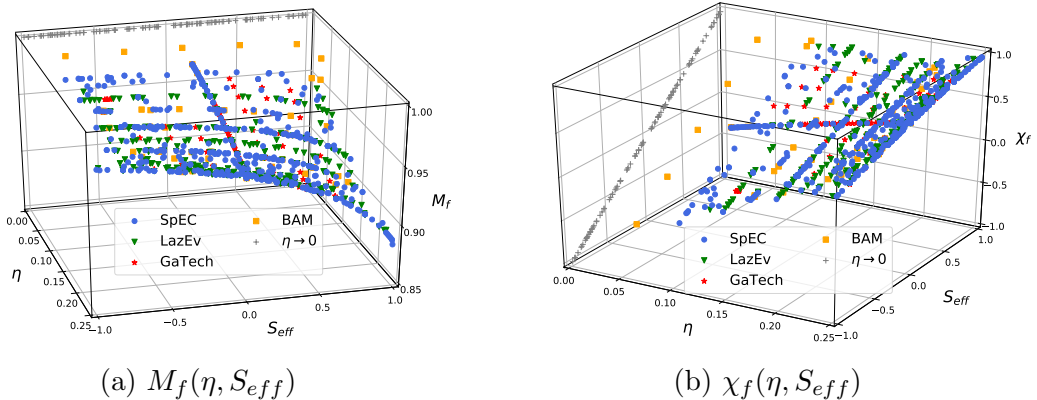


Figure 1: Final properties of the remnant BH as a function of η and S_{eff} for the non-precessing cases of Table 1. The GaTech caption corresponds to the MayaKranc code. The $\eta \rightarrow 0$ case is described in Section 2.2.

For the precessing case, the input data consisted in the full SpEC catalog, consisting in 2015 NR simulations. They cover the following parameter range: $\eta \in [0.12, 0.25]$, $\chi_1 \in [0, 0.99]$, $\chi_2 \in [0, 0.90]$, $\theta_1 \in [0, \pi]$, $\theta_2 \in [0, \pi]$, $\phi_{12} \in [0, \pi]$, $M_f \in [0.92, 0.99]$, $\chi_f \in [0.03, 0.9]$.

For the demonstration of the feasibility of the method, the parameters have been extracted for the metadata of the NR simulations for both the DNN evaluation and its comparison with the LIGO software fits [48]. The LIGO fits also includes a method to evolve the initial spins to the innermost stable circular orbit (ISCO) using post-Newtonian expression to increase the prediction agreement with the NR remnant parameters [49].

NR code	non-precessing	precessing
SpEC	592	2015
LazEv	280	0
MayaKranc	125	0
BAM	47	0
$\eta \rightarrow 0$	300	0
Total	1344	2015

Table 1: Summary of the NR simulations used to train the DNN in predicting the BH remnant properties. The $\eta \rightarrow 0$ row corresponds to the analytically known extreme mass ratio case described in Section 2.2.

2.2 Extreme mass ratio limit

In the extreme mass ratio limit of $\eta \rightarrow 0$, the BBH system can be approximated by a particle orbiting around a Kerr BH. The radiated energy and orbital momentum of the non-precessing system is known analytically [50] at the inner stable closest orbit (ISCO) as given in equations 3 and 4:

$$E_{ISCO}(\eta, \chi) = \eta \left(1 - \sqrt{\frac{2}{3\rho_{ISCO}(\chi_f)}} \right) \quad (3)$$

$$L_{ISCO}^{orb}(\eta, \chi) = \frac{2\eta \left(3\sqrt{\rho_{ISCO}(\chi)} - 2\chi \right)}{\sqrt{3\rho_{ISCO}(\chi)}} \quad (4)$$

where ρ_{ISCO} is the radius at the ISCO :

$$\begin{aligned} \rho_{ISCO}(\chi) &= 3 + Z_2 - \text{sign}(\chi) \sqrt{(3 - Z_1)(3 + Z_1 + 2Z_2)} \\ Z_1 &= 1 + (1 - \chi^2)^{1/3} \left[(1 + \chi^2)^{1/3} + (1 - \chi^2)^{1/3} \right] \\ Z_2 &= \sqrt{3\chi^2 + Z_1^2} \end{aligned}$$

The particle plunging into the BH after the ISCO, the final radiated energy is $E_{rad} = E_{ISCO}$ leading to a final mass value of $M_f = 1 - E_{ISCO}$. The final spin is obtained by solving numerically equation 5:

$$\chi_f = \frac{L_{orb} + S_1 + S_2}{M_f^2} \quad (5)$$

Following the approach in [6], we use the analytical results described above to add 300 points in the $\eta \rightarrow 0$ limit to the NR samples shown in Table 1. This additional sample enables to enhance the volume of the parameter space on which the DNN is trained, as well as better extrapolate the prediction at high mass ratio where little NR simulations are available due to the high computational cost in this regime.

3 Predicting the remnant mass and spin

3.1 Deep Neural Network

The DNN is built with the TensorFlow software version 1.13.1 [51]. The non-precessing and precessing datasets described in Section 2 are separated into three subsets: the training, validation, and testing samples containing respectively 80%, 10% and 10% of the full datasets. Each sample spans a similar range in the parameter space and is standardized in order to obtain a mean value of 0 and a standard deviation of 1 on the training dataset to

ensure a proper convergence of the algorithm. The DNN is trained on the training samples with its hyperparameters tuned heuristically, and the best hyperparameters were selected by comparing the prediction performance on the validation dataset. All DNN contains an input layer followed by four hidden layers with respectively 512, 256, 64, 32 nodes, activated by a rectified linear unit function. The last output layer ends with a linear activation function resulting in the prediction of the output value M_f or χ_f . The loss function is the mean absolute error, minimized using the adaptive stochastic gradient optimizer Adam [52]. The validation sample is not only used to select the best hyperparameters but also to avoid overfitting during the training phase, that is characterised by a decreasing loss on the training sample while all the information contained in the data have been processed into tuning the DNN. This is avoided by implementing a stopping procedure quitting the training phase when the loss is constant on the validation sample, on which the DNN is not trained. In order to ensure a correct estimation of the DNN prediction performance, the final results shown on Section 3.2 are then obtained on the testing dataset that is not used during the training and validation procedures. As DNNs are known to have limited extrapolation outside the parameter space where they have been trained, their robustness is tested by generating 10^5 BBHs with random initial parameters and verifying that the predicted remnant BH properties are below the Kerr limit.

3.2 Results

Non-precessing case The DNN correctly captures the relationship between the initial BBH parameters and the remnant properties as shown on the remnant mass and spin residual error distribution of Figure 2. We compare our results with the existing remnant mass and spin fits available in the `nrutils.py` code of the `LALInference` package of the `LALSuite` software used by the LIGO-Virgo collaborations [48]. For the non-precessing BBHs, `nrutils` includes the three-dimensional remnant fits of in [34], [13] and [6], as well as the two-dimensional fit in [12] where the spin difference is not included. The DNN improves the prediction of the final mass M_f , as the standard deviation of the absolute error distribution for the test sample is $2.6 \cdot 10^{-4}$, to compare with the range $[4, 5 \cdot 10^{-4}]$ for the other methods shown. The prediction of the final spin is similar for the remnant fits and the DNN, as the residuals root mean square (RMS) is $3 \cdot 10^{-3}$ for all three-dimensional methods. It is found to be $7 \cdot 10^{-3}$ for the two-dimensional fit in [12], indicating as expected that the initial spin difference impact the final spin value.

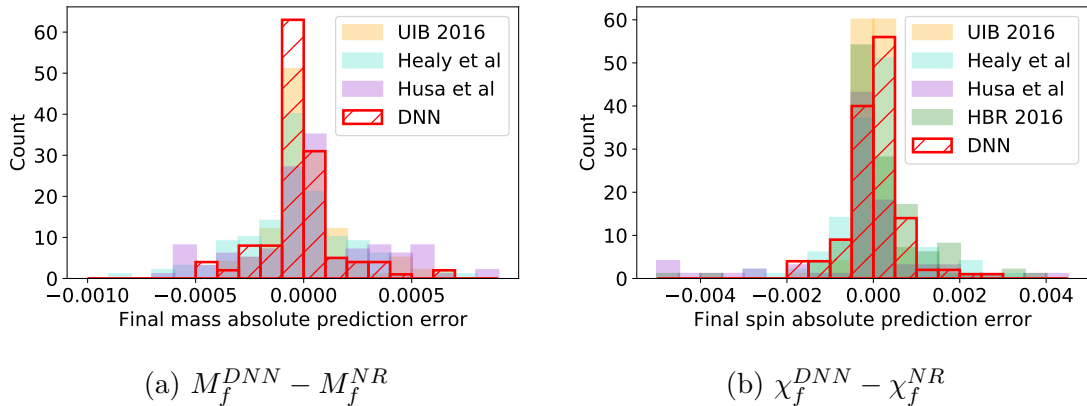


Figure 2: Residual error on the remnant mass $M_f(\eta, S_{eff}, \Delta\chi)$ (a) and spin $\chi_f(\eta, S_{eff}, \Delta\chi)$ (b) as predicted by the DNN for the non-precessing BBHs. Our error is compared with the fits performed by the UIB group in 2016 [6], Healy et al [34], Husa et al [12] and Hofmann, Barausse and Rezzolla (HBR) [13].

Precessing case The DNN predicts the remnant mass with a similar accuracy in the 6-d and 7-d parameterizations as shown on the absolute error distribution of Figure 3. The RMS of the distribution is $1 \cdot 10^{-3}$, 80% of the values have an error inferior to $1 \cdot 10^{-3}$ while the maximal absolute error is $4 \cdot 10^{-3}$. This analysis presents a generalization of the remnant mass fits to precessing binaries that is not available in the `nrutils` package, where only aligned-spins fits are available for the final mass. The package includes remnant spin fits for precessing BBHs based on aligned-spins binaries "augmented" with the in-plane spin contribution added to the final spin, as in [6], [34] and [12], and in one case an additional parameter captures the precession dynamics [13]. The currently available fits have shown to give an absolute residual error on less than 1% on the remnant mass and less than 2% on the remnant spin when using the "augmented" parameterization and spin evolution to the ISCO [49]. We compare their results on our precessing catalog with the 6d-parameterization trained DNN, as shown on Figure 4. The absolute error distribution has a RMS of $8 \cdot 10^{-3}$ for the DNN against $1.1 \cdot 10^{-2}$ for the other methods. Similarly, the prediction of the 7d-parameterization trained DNN provides a similar accuracy, demonstrating the reparameterization into the tilt angles and spin planar difference correctly captures the dynamics of precession.

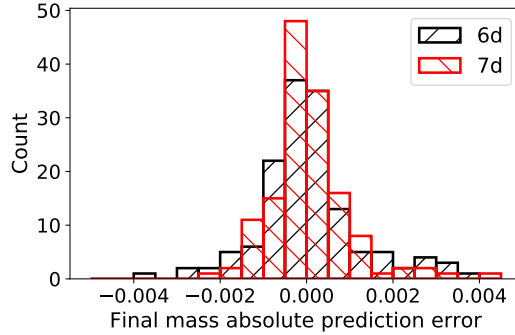


Figure 3: Residual error $M_f^{DNN} - M_f^{NR}$ on the prediction of the remnant mass for precessing BBHs. The legend refers to the 6d and 7d-parameterizations used to train the DNN.

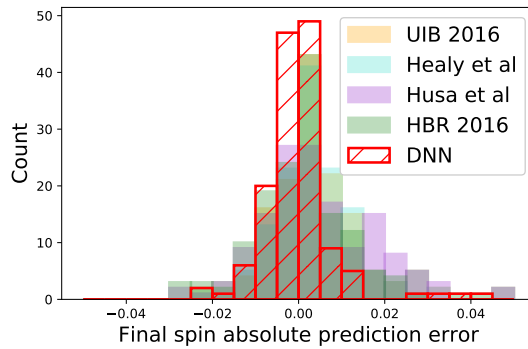


Figure 4: Residual error $\chi_f^{DNN} - \chi_f^{NR}$ on the remnant spin as predicted by the DNN for the precessing BBHs. Our error is compared with the fits performed by the UIB group in 2016 [6], Healy et al [34], Husa et al [12] and Hofmann, Barausse and Rezzolla (HBR) [13].

4 Conclusion

We demonstrate that DNNs trained on NR data are competitive with other approaches to predict the mass and spin of the remnant BH in a BBH merger, which suggests that DNN methods can be used in a similar way to more general applications in waveform modelling, e.g. to model the coefficients of a phenomenological waveform model across the parameter space, including in the presence of precession. The prediction of the final mass in the non-precessing case is about twice more accurate than the existing fits available in the public library of the LIGO software. The prediction of the final spin has a similar accuracy than the existing fits, showing that the dynamics of non-precessing BBHs are correctly captured by explicit ansatz. The DNN is shown to be a specifically powerful tool in generalizing the remnant prediction to the fully spinning case, where it provides a prediction on the final mass with an error of the order of 10^{-3} while no fit is currently available in the public LIGO software library. We also estimated the final spin magnitude for precessing binary black holes with an error of the order of 10^{-1} , and verified that the reparameterization of the projected spins used by LIGO correctly captured the precession.

The optimization of the DNN has shown that the final results have little dependency on the hyperparameters, implying that the current limitations of the prediction are due to the limited size of the NR catalogs. While our current analysis already spans a large parameter space by using all the publicly available NR catalogs, the DNN accuracy will certainly be improved as more NR simulations become available for training.

5 Acknowledgements

We thank Nathan Johnson-McDaniel and Vijay Varma for valuable discussion. This work was supported by European Union FEDER funds, the Ministry of Science, Innovation and Universities and the Spanish Agencia Estatal de Investigaci3n grants FPA2016-76821-P, RED2018-102661-T, RED2018-102573-E, FPA2017-90687-REDC, Vicepresid3ncia i Conselleria dInnovaci3, Recerca i Turisme, Conselleria dEducati3, i Universitats del Govern de les Illes Balears i Fons Social Europeu, Generalitat Valenciana (PROMETEO/2019/071), EU COST Actions CA18108, CA17137, CA16214, and CA16104, and the Swiss National Science Foundation Early Postdoc Mobility Grant 181461. The authors are grateful for computational resources provided by the LIGO Laboratory and supported by the National Science Foundation Grants PHY-0757058 and PHY-0823459.

References

- [1] A. Abramovici, W. E. Althouse, R. W. P. Drever, Y. Gursel, S. Kawamura, F. J. Raab, D. Shoemaker, L. Sievers, R. E. Spero, K. S. Thorne, R. E. Vogt, R. Weiss, S. E. Whitcomb, and M. E. Zucker. LIGO - The Laser Interferometer Gravitational-Wave Observatory. *Science*, 256:325–333, April 1992.
- [2] B. P. Abbott et al. GW150914: The Advanced LIGO Detectors in the Era of First Discoveries. *Phys. Rev. Lett.*, 116(13):131103, 2016.
- [3] F. Acernese et al. Advanced Virgo: a second-generation interferometric gravitational wave detector. *Class. Quant. Grav.*, 32(2):024001, 2015.
- [4] B. P. Abbott et al. GWTC-1: A Gravitational-Wave Transient Catalog of Compact Binary Mergers Observed by LIGO and Virgo during the First and Second Observing Runs. 2018.
- [5] Luc Blanchet. Gravitational radiation from post-newtonian sources and inspiralling compact binaries. *Living Reviews in Relativity*, 17(1), Feb 2014.
- [6] Xisco Jimnez-Forteza, David Keitel, Sascha Husa, Mark Hannam, Sebastian Khan, and Michael Prrer. Hierarchical data-driven approach to fitting numerical relativity data for nonprecessing binary black holes with an application to final spin and radiated energy. *Phys. Rev.*, D95(6):064024, 2017.
- [7] Mark Hannam, Patricia Schmidt, Alejandro Boh, Lela Haegel, Sascha Husa, Frank Ohme, Geraint Pratten, and Michael Prrer. Simple Model of Complete Precessing Black-Hole-Binary Gravitational Waveforms. *Phys. Rev. Lett.*, 113(15):151101, 2014.
- [8] Sebastian Khan, Sascha Husa, Mark Hannam, Frank Ohme, Michael Prrer, Xisco Jimnez Forteza, and Alejandro Boh. Frequency-domain gravitational waves from nonprecessing black-hole binaries. II. A phenomenological model for the advanced detector era. *Phys. Rev.*, D93(4):044007, 2016.
- [9] B. P. Abbott et al. Tests of General Relativity with the Binary Black Hole Signals from the LIGO-Virgo Catalog GWTC-1. 2019.
- [10] Yann LeCun, Yoshua Bengio, and Geoffrey Hinton. Deep learning. *nature*, 521(7553):436, 2015.

- [11] Vijay Varma, Davide Gerosa, François Hébert, Leo C. Stein, and Hao Zhang. High-accuracy mass, spin, and recoil predictions of generic black-hole merger remnants. 2018.
- [12] Sascha Husa, Sebastian Khan, Mark Hannam, Michael Prer, Frank Ohme, Xisco Jimnez Forteza, and Alejandro Boh. Frequency-domain gravitational waves from nonprecessing black-hole binaries. I. New numerical waveforms and anatomy of the signal. *Phys. Rev.*, D93(4):044006, 2016.
- [13] Fabian Hofmann, Enrico Barausse, and Luciano Rezzolla. The final spin from binary black holes in quasi-circular orbits. *The Astrophysical Journal Letters*, 825(2):L19, 2016.
- [14] <http://www.black-holes.org/waveforms>.
- [15] Tony Chu, Harald P. Pfeiffer, and Mark A. Scheel. High accuracy simulations of black hole binaries: Spins anti-aligned with the orbital angular momentum. *Phys. Rev.*, D80:124051, 2009.
- [16] Geoffrey Lovelace, Mark.A. Scheel, and Bela Szilagyi. Simulating merging binary black holes with nearly extremal spins. *Phys. Rev.*, D83:024010, 2011.
- [17] Geoffrey Lovelace, Michael Boyle, Mark A. Scheel, and Bela Szilagyi. Accurate gravitational waveforms for binary-black-hole mergers with nearly extremal spins. *Class. Quant. Grav.*, 29:045003, 2012.
- [18] Luisa T. Buchman, Harald P. Pfeiffer, Mark A. Scheel, and Bela Szilagyi. Simulations of non-equal mass black hole binaries with spectral methods. *Phys. Rev.*, D86:084033, 2012.
- [19] Abdul H. Mroue and Harald P. Pfeiffer. Precessing Binary Black Holes Simulations: Quasicircular Initial Data. 2012.
- [20] Daniel A. Hemberger, Geoffrey Lovelace, Thomas J. Loredo, Lawrence E. Kidder, Mark A. Scheel, Bela Szilagyi, Nicholas W. Taylor, and Saul A. Teukolsky. Final spin and radiated energy in numerical simulations of binary black holes with equal masses and equal, aligned or anti-aligned spins. *Phys. Rev.*, D88:064014, 2013.
- [21] Ian Hinder et al. Error-analysis and comparison to analytical models of numerical waveforms produced by the NRAR Collaboration. *Class. Quant. Grav.*, 31:025012, 2014.

- [22] Abdul H. Mroue et al. Catalog of 174 Binary Black Hole Simulations for Gravitational Wave Astronomy. *Phys. Rev. Lett.*, 111(24):241104, 2013.
- [23] Geoffrey Lovelace et al. Nearly extremal apparent horizons in simulations of merging black holes. *Class. Quant. Grav.*, 32(6):065007, 2015.
- [24] Mark A. Scheel, Matthew Giesler, Daniel A. Hemberger, Geoffrey Lovelace, Kevin Kuper, Michael Boyle, B. Szilagyi, and Lawrence E. Kidder. Improved methods for simulating nearly extremal binary black holes. *Class. Quant. Grav.*, 32(10):105009, 2015.
- [25] Jonathan Blackman, Scott E. Field, Chad R. Galley, Bela Szilagyi, Mark A. Scheel, Manuel Tiglio, and Daniel A. Hemberger. Fast and Accurate Prediction of Numerical Relativity Waveforms from Binary Black Hole Coalescences Using Surrogate Models. *Phys. Rev. Lett.*, 115(12):121102, 2015.
- [26] Prayush Kumar, Kevin Barkett, Swetha Bhagwat, Nousha Afshari, Duncan A. Brown, Geoffrey Lovelace, Mark A. Scheel, and Bela Szilagyi. Accuracy and precision of gravitational-wave models of inspiraling neutron star-black hole binaries with spin: Comparison with matter-free numerical relativity in the low-frequency regime. *Phys. Rev.*, D92(10):102001, 2015.
- [27] Tony Chu, Heather Fong, Prayush Kumar, Harald P. Pfeiffer, Michael Boyle, Daniel A. Hemberger, Lawrence E. Kidder, Mark A. Scheel, and Bela Szilagyi. On the accuracy and precision of numerical waveforms: Effect of waveform extraction methodology. *Class. Quant. Grav.*, 33(16):165001, 2016.
- [28] Geoffrey Lovelace et al. Modeling the source of GW150914 with targeted numerical-relativity simulations. *Class. Quant. Grav.*, 33(24):244002, 2016.
- [29] B. P. Abbott et al. GW151226: Observation of Gravitational Waves from a 22-Solar-Mass Binary Black Hole Coalescence. *Phys. Rev. Lett.*, 116(24):241103, 2016.
- [30] B. P. Abbott et al. Directly comparing GW150914 with numerical solutions of Einsteins equations for binary black hole coalescence. *Phys. Rev.*, D94(6):064035, 2016.
- [31] Benjamin P. Abbott et al. Effects of waveform model systematics on the interpretation of GW150914. 2016.

- [32] Vijay Varma, Scott Field, Mark A. Scheel, Jonathan Blackman, Lawrence E. Kidder, and Harald P. Pfeiffer. Surrogate model of hybridized numerical relativity binary black hole waveforms. 2018.
- [33] Michael Boyle, Daniel Hemberger, Dante A B Iozzo, Geoffrey Lovelace, Serguei Ossokine, Harald P Pfeiffer, Mark A Scheel, Leo C Stein, Charles J Woodford, Aaron B Zimmerman, and et al. The sxs collaboration catalog of binary black hole simulations. *Classical and Quantum Gravity*, 36(19):195006, Sep 2019.
- [34] James Healy, Carlos O. Lousto, and Yosef Zlochower. Remnant mass, spin, and recoil from spin aligned black-hole binaries. *Phys. Rev. D*, 90:104004, Nov 2014.
- [35] Carlos O. Lousto and James Healy. Flip-flopping binary black holes. *Phys. Rev. Lett.*, 114:141101, Apr 2015.
- [36] Hiroyuki Nakano, James Healy, Carlos O. Lousto, and Yosef Zlochower. Perturbative extraction of gravitational waveforms generated with numerical relativity. *Phys. Rev. D*, 91:104022, May 2015.
- [37] Carlos O. Lousto, James Healy, and Hiroyuki Nakano. Spin flips in generic black hole binaries. *Phys. Rev. D*, 93:044031, Feb 2016.
- [38] Carlos O. Lousto and James Healy. Unstable flip-flopping spinning binary black holes. *Phys. Rev. D*, 93:124074, Jun 2016.
- [39] James Healy and Carlos O. Lousto. Remnant of binary black-hole mergers: New simulations and peak luminosity studies. *Phys. Rev. D*, 95:024037, Jan 2017.
- [40] James Healy, Carlos O. Lousto, and Yosef Zlochower. Nonspinning binary black hole merger scenario revisited. *Phys. Rev. D*, 96:024031, Jul 2017.
- [41] James Healy, Carlos O Lousto, Hiroyuki Nakano, and Yosef Zlochower. Post-newtonian quasicircular initial orbits for numerical relativity. *Classical and Quantum Gravity*, 34(14):145011, jun 2017.
- [42] J. Healy, J. Lange, R. O’Shaughnessy, C. O. Lousto, M. Campanelli, A. R. Williamson, Y. Zlochower, J. Calderón Bustillo, J. A. Clark, C. Evans, D. Ferguson, S. Ghonge, K. Jani, B. Khamesra, P. Laguna, D. M. Shoemaker, M. Boyle, A. García, D. A. Hemberger, L. E. Kidder, P. Kumar, G. Lovelace, H. P. Pfeiffer, M. A. Scheel, and S. A. Teukolsky. Targeted numerical simulations of binary black holes for gw170104. *Phys. Rev. D*, 97:064027, Mar 2018.

- [43] James Healy, Carlos O. Lousto, Ian Ruchlin, and Yosef Zlochower. Evolutions of unequal mass, highly spinning black hole binaries. *Phys. Rev. D*, 97:104026, May 2018.
- [44] James Healy and Carlos O. Lousto. Hangup effect in unequal mass binary black hole mergers and further studies of their gravitational radiation and remnant properties. *Phys. Rev. D*, 97:084002, Apr 2018.
- [45] Karan Jani, James Healy, James A Clark, Lionel London, Pablo Laguna, and Deirdre Shoemaker. Georgia tech catalog of gravitational waveforms. *Classical and Quantum Gravity*, 33(20):204001, sep 2016.
- [46] Bernd Bruegmann, Jose A. Gonzalez, Mark Hannam, Sascha Husa, Ulrich Sperhake, and Wolfgang Tichy. Calibration of Moving Puncture Simulations. *Phys. Rev.*, D77:024027, 2008.
- [47] Sascha Husa, Jose A. Gonzalez, Mark Hannam, Bernd Bruegmann, and Ulrich Sperhake. Reducing phase error in long numerical binary black hole evolutions with sixth order finite differencing. *Class. Quant. Grav.*, 25:105006, 2008.
- [48] LIGO Scientific Collaboration. LIGO Algorithm Library - LALSuite. free software (GPL), 2018.
- [49] N. K. Johnson-McDaniel et al. Determining the final spin of a binary black hole system including in-plane spins: Method and checks of accuracy. Technical Report LIGO Document T1600168-v6, 2016.
- [50] James M Bardeen, William H Press, and Saul A Teukolsky. Rotating black holes: locally nonrotating frames, energy extraction, and scalar synchrotron radiation. *The Astrophysical Journal*, 178:347–370, 1972.
- [51] Martín Abadi, Ashish Agarwal, Paul Barham, Eugene Brevdo, Zhifeng Chen, Craig Citro, Greg S. Corrado, Andy Davis, Jeffrey Dean, Matthieu Devin, Sanjay Ghemawat, Ian Goodfellow, Andrew Harp, Geoffrey Irving, Michael Isard, Yangqing Jia, Rafal Jozefowicz, Lukasz Kaiser, Manjunath Kudlur, Josh Levenberg, Dandelion Mané, Rajat Monga, Sherry Moore, Derek Murray, Chris Olah, Mike Schuster, Jonathon Shlens, Benoit Steiner, Ilya Sutskever, Kunal Talwar, Paul Tucker, Vincent Vanhoucke, Vijay Vasudevan, Fernanda Viégas, Oriol Vinyals, Pete Warden, Martin Wattenberg, Martin Wicke, Yuan Yu, and Xiaoqiang Zheng. TensorFlow: Large-scale machine learning on heterogeneous systems, 2015. Software available from tensorflow.org.
- [52] Diederik P Kingma and Jimmy Ba. Adam: A method for stochastic optimization. *arXiv preprint arXiv:1412.6980*, 2014.